

Effect of Spatial and Temporal Traffic Statistics on the Performance of Wireless Networks

Gang Wang, Yi Zhong, *Member, IEEE*, Rongpeng Li, *Member, IEEE*, Xiaohu Ge, *Senior Member, IEEE*, Tony Q.S. Quek, *Fellow, IEEE* and Guoqiang Mao, *Fellow, IEEE*

Abstract—The traffic in wireless networks has become diverse and fluctuating both spatially and temporally due to the emergence of new wireless applications and the complexity of scenarios. The purpose of this paper is to quantitatively analyze the impact of the wireless traffic, which fluctuates both spatially and temporally, on the performance of the wireless networks. Specially, we propose to combine the tools from stochastic geometry and queueing theory to model the spatial and temporal fluctuation of traffic, which to our best knowledge has seldom been evaluated analytically. We derive the spatial and temporal statistics, the total arrival rate, the stability of queues and the delay of users by considering two different spatial properties of traffic, i.e., the uniformly and non-uniformly distributed cases. The numerical results indicate that although the fluctuation of traffic (reflected by the variance of total arrival rate) when the users are clustered is much fiercer than that when the users are uniformly distributed, the stability performance is much better. Our work provides a useful reference for the design of wireless networks when the complex spatio-temporal fluctuation of the traffic is considered.

Index Terms—Traffic, delay, queueing theory, stability, stochastic geometry

I. INTRODUCTION

A. Motivations

The emergence of various smart devices and wireless applications, such as real-time wireless gaming, smart grid, free-viewpoint video, advanced manufacturing and Tactile Internet [2], [3], has led to diversified traffic and quality-of-service (QoS) requirements. For example, the voice traffic in the wireless networks is typically delay-sensitive and symmetric in uplink and downlink, while the data and video traffic are generally loss-sensitive and asymmetric in uplink and downlink, which are IP-based and can tolerate certain delay [4]. A meaningful and practically relevant problem is to meet the QoS requirements of diversified applications, which is also one of the most significant goals for the 5G wireless networks.

With the continuous evolution of wireless networks, the tremendous traffic and its dynamic variations have become

more and more significant in affecting the performance of wireless networks. The pattern of the traffic in a wireless network determines whether a resource block of a base station (BS) is occupied or not, which then shapes the interference pattern in the wireless network. The interference pattern, in turn, affects the performance of the transceiver links in the wireless network, which directly determines the service process of the traffic. Therefore, the traffic and the service provided by the wireless networks are highly coupled with each other. Modeling and analysis of the traffic are essential to design and configure the wireless networks so as to match the network service with the traffic [5].

The spatial distribution and the temporal variation of wireless traffic are much more complicated than before. For example, in a cellular network, the wireless traffic during a holiday or a weekend is generally lighter than that during a weekday, and the traffic during the midnight is generally lighter than that during the day time. Meanwhile, the spatial distributions of the wireless traffic are also very different between different regions. For example, the traffic in the business regions could be much heavier during the day time than that during the midnight, and it is reversed in the residential region. The integrated analysis of the traffic with spatial and temporal fluctuation requires to appropriately model both the spatial distribution and the temporal variation of the traffic in the wireless networks. Although the effect of the wireless traffic has been studied extensively, most of them only consider one aspect of the traffic [6]–[8]. The works only modeling the spatial distribution usually use the tools from the stochastic geometry and model the spatial distribution of users by either the uniform (such as the Poisson point process (PPP)) or the non-uniform point processes. Other works only modeling the temporal variations of traffic usually use the queueing theory to model the arrival process of the packets as stochastic processes. To model both aspects of the traffic, which is necessary for analyzing the wireless networks, requires the combination of stochastic geometry and queueing theory, which brings in more complexities and difficulties in the modeling and evaluation.

B. Related Works

Related works are summarized as follows. The authors in [6], [7] discussed the patterns and the spatio-temporal characteristics of wireless traffic in the practical cellular networks. In [6], the authors presented the analysis of traffic measurements collected from commercial cellular networks in

Gang Wang, Yi Zhong and Xiaohu Ge are with School of Electronic Information and Communications, Huazhong University of Science and Technology, Wuhan, P. R. China. Rongpeng Li is with Zhejiang University, Hangzhou, China. Tony Q.S. Quek is with Information Systems Technology and Design, Singapore University of Technology and Design, Singapore. Guoqiang Mao is with School of Electrical and Data Engineering, University of Technology Sydney, Sydney, Australia.

This research was supported by the National Natural Science Foundation of China (NSFC) grants No. 61701183 and No. 61701439. Part of this work was presented at the 2018 IEEE Global Communications Conference (GLOBECOM) [1].

The corresponding author is Yi Zhong (e-mail: yzhong@hust.edu.cn).

China and proposed a spatial traffic model which generated large-scale spatial traffic variations by a sum of sinusoids. In [7], the authors quantitatively characterized the spatio-temporal distribution of mobile traffic and presented a detailed visualized analysis, and the work [9] revealed that the traffic is typically unbalanced, changing not only in the time domain but also in the spatial domain. In [10], the authors extracted and modeled the traffic patterns of large scale towers deployed in a metropolitan city. In [11], the authors showed some cell phone activity patterns based on the cell phone data which consists of telecommunications activity records in the city of Milan from Telecom Italia Mobile, and the patterns demonstrated that the mobile traffic of urban ecology were clustered in both the time domain and the spatial domain. The above works reveal that both the spatial distribution and the temporal variation of traffic are irregular, and there is a clear need for new analytical methods to explore the properties of irregular distributions and variations of the up-to-date wireless traffic.

Theoretical analysis of the spatial properties of the wireless traffic is generally based on the stochastic geometry. In [12], the probability density function (PDF) of the number of users in each Voronoi cell was derived by modeling the locations of users as a homogeneous PPP. The works [13], [14] extended such PDFs to the case of multi-tier heterogeneous networks. In [13], the authors analyzed the effect of the offloading traffic in heterogeneous networks on the system performance and the authors in [14] developed a framework to characterize the signal-to-noise-plus-interference ratio (SINR) in a heterogeneous cellular network. In [15], the authors considered a single-tier uplink Poisson cellular network and analyzed the meta distribution of the SIR for both the cellular network uplink and downlink with fractional power control. In [16], [17], the authors summarized the applications of the point processes in wireless networks, where the average behavior over many spatial realizations of a network can be evaluated appropriately. In [18], the authors proposed a model to capture the coupling between users and small cell base stations by using tools from stochastic geometry. In [19], the authors compared the traditional square grid model with the PPP model in terms of coverage, and they discussed the average achievable rate in the general case. As for the temporal arrival of packets, the analysis was generally based on the queueing theory. In [20], the authors considered a shared access network with one primary source-destination pair and many secondary communication pairs and they discussed secondary throughput optimization with primary delay constraints by using tools from stochastic geometry and queueing theory. In [21], the authors investigated the effect of bursty traffic and analyzed the delay and throughput in a wireless caching system by using queueing theory. The queueing delay was analyzed with a random access network in [22]. In [23]–[27], a discrete-time slotted ALOHA system with multiple terminals was described, where each terminal had an infinite buffer to store the packets. In [28]–[30], the energy efficiency is evaluated by considering the random cellular networks.

The works modeling both the spatial and temporal aspects of the wireless traffic include [31] and [32], where the authors simultaneously modeled the spatio-temporal arrival of traffic and

considered the traffic generated at random spatial regions. In [33], the authors discussed three kinds of scheduling policies, i.e., the random scheduling, the first-input-first-output (FIFO) scheduling and the round-robin scheduling, and compared the delay performance under different scheduling policies. In [34], the authors developed a traffic-aware spatio-temporal mathematical model for Internet of Things (IoT) devices supported by cellular uplink connectivity and discussed the stability for three transmission strategies. In [35], the authors analyzed the random access channel in cellular-based massive IoT networks based on a traffic-aware spatio-temporal model, where the spatial topology was modeled based on stochastic geometry and the queue evolution was analyzed based on probability theory. In [36], the authors proposed a user-centric mobility management to cope with user spatial movement and temporally correlated wireless channels in ultra-dense cellular. In [37], the authors evaluated the tradeoff between delay and physical layer security. In [38], the authors combined stochastic geometry and queueing theory to describe the network with spatial irregularity and temporal evolution. However, the non-uniform property of network and the various temporal arrival processes of traffic are not considered.

C. Contributions

In this paper, we establish a tractable model to characterize both the spatial distribution and the temporal variation of traffic in wireless networks. The spatial distribution of traffic could be described by the locations of users. Ignoring the mobility of users, the temporal variation of traffic is described by a random arrival process of packets for each user and the dynamic serving process of arrived packets. We consider two different packet arrival rate distributions, i.e., uniform distribution and exponential distribution. Considering both the uniformly distributed traffic modeled by a PPP and the non-uniformly distributed traffic modeled by a Poisson cluster process (PCP), we explore the relationship between traffic and delay to gain insight. The main contributions of this paper are summarized as follows.

- Analytical framework based on combining stochastic geometry and queueing theory is proposed to qualitatively evaluate the spatial and temporal fluctuation of the wireless traffic.
- The spatial and temporal statistics of traffic, the stability of queues and the delay are derived for uniformly and non-uniformly distributed traffic. The numerical analyses based on the theoretical results are investigated to gain insights.
- The effect of various parameters of the traffic is discussed in terms of meeting the delay and stability requirements. Our results reveal that although the fluctuation of traffic (reflected by the variance of total arrival rate) when the users are clustered is much fiercer than that when the users are uniformly distributed, the stability performance is much better.

The remaining part of the paper is organized as follows. In Section II, we describe the system models. Then, we study the statistics of traffic and derive the success probability,

TABLE I
NOTATIONS USED IN THIS PAPER

Notation	Definition
Φ_b	PPP of the BSs with density λ_b
Φ_u	Point process of the users with density λ_u
P_b	Transmission power
Φ_p	Parent point process of the parent points with density λ_p
Φ_x	Daughter point process ($x \in \Phi_p$) with density λ_c
r_c	Radius of the user cluster
ξ_i	Arrival rate of packets at the user x_i
β	Mean delay requirement
h_0	Fading coefficient of the desired link
g_i	Fading coefficient of the interference link from the BS y_i
l_0	Distance between the typical user and its associated BS
L_i	Distance between the typical user and the interfering BS y_i
α	Path loss exponent
θ	Threshold of SIR
\mathbf{P}_s	Success probability
δ	α -related constant, defined as $\delta = 2/\alpha$
τ	Achievable rate of the typical user

achievable rate, delay and unstable probability in Section III, IV and V. Numerical results are given in Section VI. Finally, Section VII concludes the paper. The notations are listed in Table I.

II. SYSTEM MODEL

A. Network Structure

We first show the spatial and temporal distribution of the wireless traffic in the real scenarios. The data sets are based on a large number of practical traffic records from China Mobile in Hangzhou, an eastern provincial capital in China via the Gb interface of 2G/3G cellular networks or S1 interface of 4G cellular networks [39]. Figure 1 shows the traffic amount for three different applications during one day in the randomly selected cells, which is consistent with the experiments in [8]. In Figure 2, we plot the traffic density of three kinds of typical applications, i.e., instant messaging (IM), web browsing and video, at 9AM and 3PM in randomly selected dense urban areas. As shown in Figure 2, there are some “hot spots” varying in both temporal and spatial domain, and the spatially clustering property is also consistent with the experiments in [8]. Based on the characteristics of the real traffic in these figures, we propose an analytical model and study the effect of the traffic on the performance of wireless networks.

We consider a wireless network that consists of one tier of BSs and one tier of users, as illustrated in Figure 3. In this paper, we discuss the downlink of the wireless network with ALOHA channel access. The locations of BSs are modeled as a homogeneous PPP $\Phi_b = \{y_i\}$ with intensity λ_b , denoted by $\Phi_b \sim \text{PPP}(\lambda_b)$. The users are modeled by another point process $\Phi_u = \{x_i\}$. The transmission power of the BSs is P_b . Since the network considered in the work is a single tier network, the shared spectrum policy is reasonable. The users in the network are shared with the same spectrum resource.

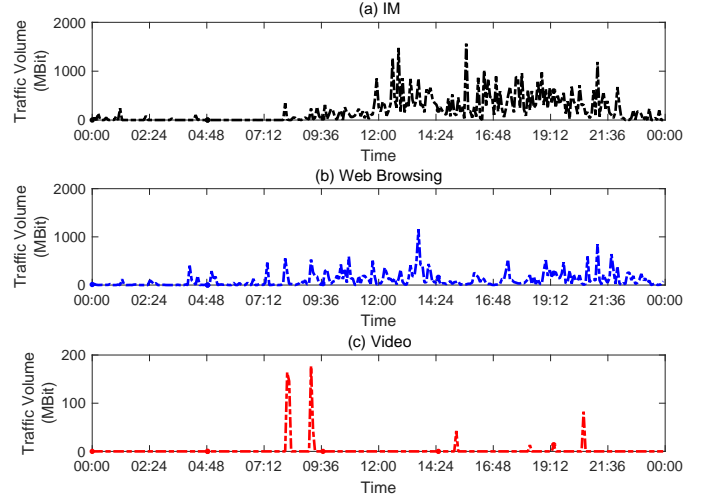


Fig. 1. The volume of cellular traffic of three different applications during one day in the randomly selected cells.

In the time domain, the time is slotted into discrete time slots and the users will acquire the dominant right of the time slot with a random probability at each time slot. We consider the following two kinds of spatial distributions for the users.

- Case 1: The locations of users form a homogeneous PPP of intensity λ_u as shown in the left graph in Figure 3.
- Case 2: The locations of users are distributed as a PCP as shown in the right graph in Figure 3. The centers of the clusters, i.e., the parent points, are distributed according to a PPP Φ_p of intensity λ_p . The users are uniformly scattered according to an independent PPP Φ_x of intensity λ_c in the circular covered area of radius r_c centered at each parent point $x \in \Phi_p$, which are called the daughter points. Thus, the distribution of all users is

$$\Phi_u = \bigcup_{x \in \Phi_p} \Phi_x. \quad (1)$$

In this case, the number of users in the typical cluster is a Poisson random variable with parameter $\pi r_c^2 \lambda_c$, and the intensity of all users is $\lambda_u = \pi r_c^2 \lambda_c \lambda_p$.

We assume that the packets arrival process for each user $x_i \in \Phi_u$ is an independent Bernoulli process [23], [33]. The packet arrival rate is denoted by ξ and ξ_i is the probability of a packet arriving at the user x_i in any time slot. Since the locations and states of users are independent and identical in our model, in order to analyze the network performance conveniently, we randomly select a user as the typical user and the location of the typical user is assumed to be at the origin. The BS associated with the typical user is regarded as the typical BS. Obviously, the packet arrival rates of users $\{\xi_i\}$ are independently and identically distributed (i.i.d.) random variables. The size of each packet is assumed to be fixed, and a BS requires exactly one time slot to deliver one packet. Each BS maintains an independent buffer of infinite size for each user within its coverage to save the incoming packets. The number of queues at each BS equals to the number of users within the coverage of the BS. If the transmission of a

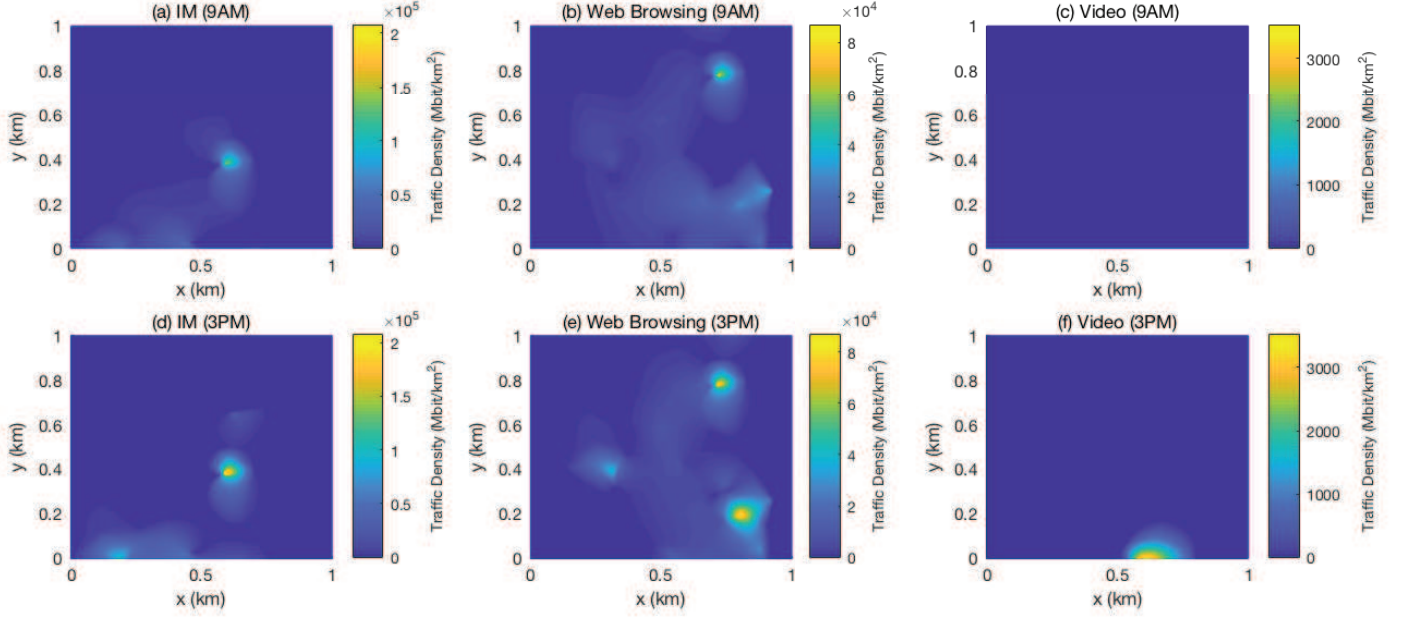


Fig. 2. The density of cellular traffic of three wireless applications, i.e., instant messaging (IM), web browsing and video, at 9AM and 3PM in the randomly selected dense urban areas.

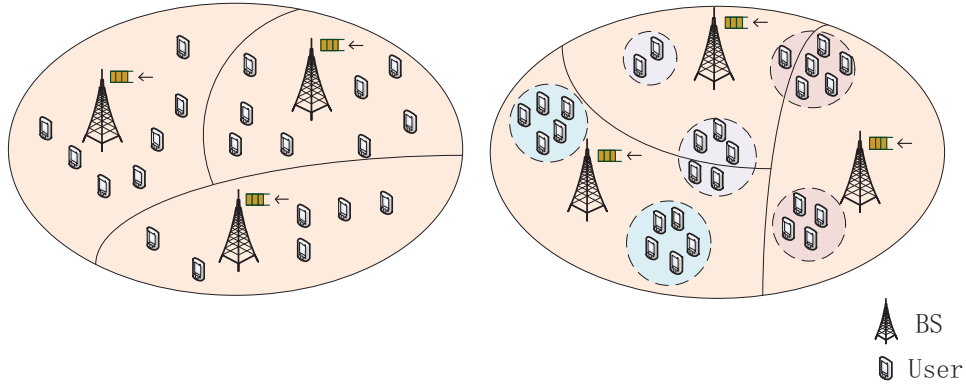


Fig. 3. Illustration of the network model with BSs and users. Uniformly distributed traffic is modeled by the PPP in the left graph and non-uniformly distributed traffic is modeled by the PCP in the right graph.

packet is failed, it will be added into the head of queue and be transmitted again.

The delay requirement is the maximum delay that a user can tolerate, and the delay requirements for different users are different. Considering the various delay requirements, we assume that the mean delay requirement β can be equal to three levels, i.e., small value β_s , medium value β_m and large value β_l , which correspond to the strict delay requirement, medium delay requirement and loose delay requirement respectively.

B. Channel and SIR

Considering the propagation loss, we assume that the links between the serving BS and the users experience Rayleigh fading with unit mean. Then, the received signal power of a user at a distance l from its serving BS is $P_b h l^{-\alpha}$ where $h \sim \text{Exp}(1)$.

In other words, the power fading coefficients in different time slots are i.i.d. random variables and keep constant during one time slot. The fading coefficients of interference links are denoted by $\{g_i\}$. Since the noise is not the most focused and interested factor of our work and the network considered in the study consists of one tier of BSs and one tier of users where the interference from interfering BSs are more influential than the noise on the network performance, we ignore the noise power in the analysis. If the signal-to-interference ratio (SIR) at a user is larger than a constant threshold θ , the receiver can successfully decode the packets. Otherwise, the packet will be failed for decoding, and the failed packets will be added into the head of the queues and wait to be scheduled again.

Without loss of generality, we introduce the random scheduling in which each user is served randomly by the associated BS with equal probability. We assume that the users

always access their nearest BSs. The typical user is assumed to be located at the origin, and its serving BS is located at y_0 . Note that we consider the downlink in this paper. Let l_0 be the distance between the typical user and its associated BS y_0 , and $\{L_i\}$ be the distances between the typical user and the interfering BSs. The SIR of the typical user with a distance l_0 from its serving BS is

$$\text{SIR} = \frac{P_b h_0 l_0^{-\alpha}}{\sum_{y_i \in \Phi_b \setminus y_0} P_b g_i L_i^{-\alpha}}. \quad (2)$$

III. TRAFFIC STATISTIC

In order to evaluate the spatial and temporal fluctuation of the traffic, we consider two metrics, i.e., the probability distribution of the number of users served by a BS and the variance of total arrival rate. We first introduce the following lemma.

Lemma 1. *The PDF of the coverage area S of a BS is approximated as [12], [40]*

$$f_S(x) \simeq \frac{343}{15} \sqrt{\frac{3.5}{\pi}} (x \lambda_b)^{2.5} \exp(-3.5 x \lambda_b) \lambda_b. \quad (3)$$

Proof: In [12], the authors give the approximate PDF of the size of a macro-cell coverage area and the detailed mathematical derivations and simulations can refer to [40]. ■

Firstly, we derive the probability mass function (PMF) of the number of users for the uniformly distributed traffic where the users are modeled by a homogeneous PPP.

Lemma 2. *Let N be the number of users in a cell with given area S when the users form a PPP. The PMF of N is [17]*

$$\mathbb{P}(N = k) = \frac{e^{-(\lambda_u S)}}{k!} (\lambda_u S)^k. \quad (4)$$

Proof: The PMF of N is obtained by the definition of two-dimensional PPP and the author gives detailed mathematical derivations and descriptions of general PPP in [17, ch.2]. ■

For the case of non-uniformly distributed traffic where the users are distributed as a PCP, the users access to the nearest BSs. Then, we get the following lemma.

Lemma 3. *Let N be the number of users in a cell with given area S when the users are distributed as a PCP. The PMF of N is*

$$\begin{aligned} \mathbb{P}(N = k) &= \sum_{a=0}^{\infty} \mathbb{P}(N_p = a, N_d = k) \\ &= \sum_{a=0}^{\infty} \frac{e^{-\lambda_p S}}{a!} \left(\lambda_p S e^{-\lambda_c \pi r_c^2} \right)^a \frac{(\lambda_c a \pi r_c^2)^k}{k!}, \end{aligned} \quad (5)$$

where N_p is the number of parent points, and N_d is the number of daughter points.

Proof: Note that each user always access the nearest BS, which may lead to the case that some users belong to the same cluster access to different BSs. In order to obtain the PMF of the number of users in Lemma 3, we approximately assume that all users in the same cluster always access to

the same BS, which is the nearest one to the parent point of that cluster. To verify the accuracy of this assumption, we compare the numerical results obtained from approximation and the simulation results.

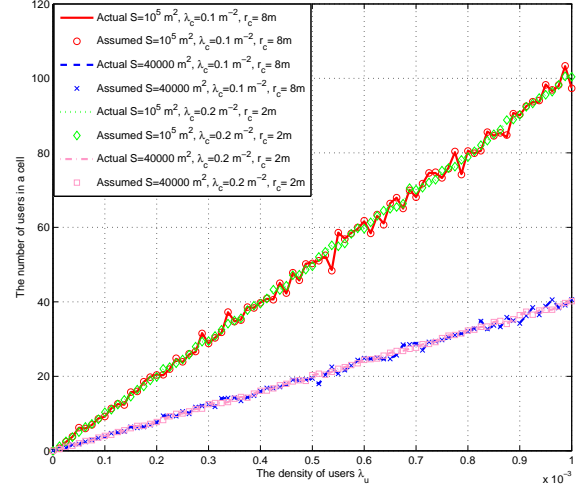


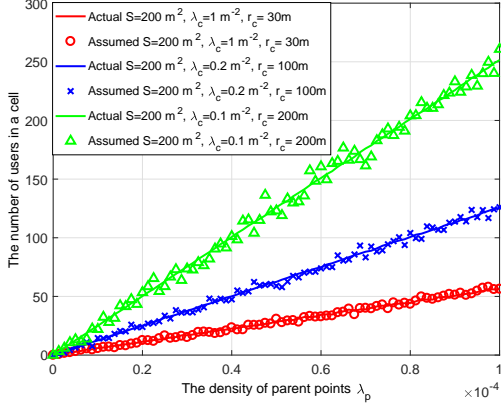
Fig. 4. Number of users in a cell as functions of λ_u when the users form a PCP with given area S .

In Figure 4 and Figure 5, the curves ‘Actual’ denote the actual number of users when each user accesses the nearest BSs. The curves ‘Assumed’ denote the number of users when all users belong to the same cluster access the same BS which is the nearest one to the parent point of that cluster. In particular, we plot the ‘Actual’ and ‘Assumed’ curves for different cell areas S and various PCP parameters to verify the accuracy of the assumption. It is observed that the ‘Assumed’ curve approaches to the ‘Actual’ curve, indicating that the approximation is reasonable. Thus, we get the PMF of N based on this approximation as

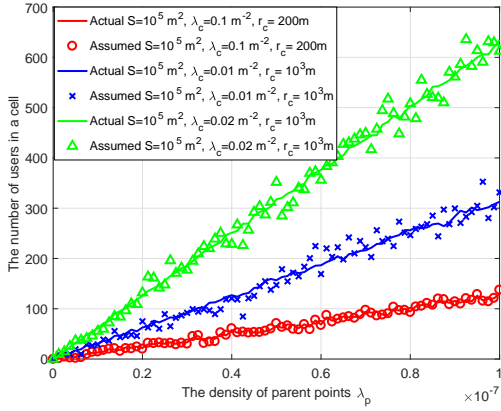
$$\begin{aligned} \mathbb{P}(N = k) &\stackrel{(a)}{=} \sum_{a=0}^{\infty} \mathbb{P}(N_p = a) \mathbb{P}(N_d = k | N_p = a) \\ &= \sum_{a=0}^{\infty} \frac{e^{-\lambda_p S}}{a!} \left(\lambda_p S e^{-\lambda_c \pi r_c^2} \right)^a \frac{(\lambda_c a \pi r_c^2)^k}{k!}, \end{aligned} \quad (6)$$

where (a) follows from the total probability formula. ■

In Figure 6, we plot the PMF of the number of users in the cases where the users form a PPP or a PCP with the same λ_u in a cell with area S . We observe that, with given cell area S , the probability that the number of users is either very small or very large in the PCP case is larger than that in the PPP case. This is partly attributed to the fact that the users in the PCP case appear to be more grouped. Meanwhile, the PMF in the PPP case is more centralized so the probability is larger than that in the PCP case when the number of users is a medium value. In both cases, as the value of $\lambda_u S$ increases gradually, the peak value of the PMF decreases since the PMF is more dispersed when the mean number of users increases. As shown in circle 1, the number of users increases due to the increase of the mean number of users $\lambda_u S$.



(a) Small cell size results



(b) Large cell size results

Fig. 5. Number of users in a cell as functions of λ_p when the users form a PCP with given area S .

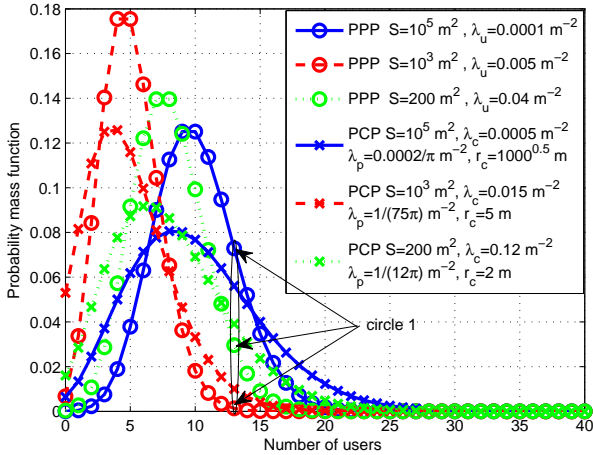


Fig. 6. The PMF of the number of users when the users form a PPP or a PCP with the same λ_u and given area S .

Let $\xi_{j,\text{total}}$ be the total arrival rate of packets in the coverage area S_j of a BS y_j , we get

$$\xi_{j,\text{total}} = \sum_{x_i \in \Phi_{u,S_j}} \xi_i, \quad (7)$$

where Φ_{u,S_j} is the set of users in area S_j . N_j is the total number of users in area S_j . The mean total arrival rate in area S_j , $\mathbb{E}[\xi_{j,\text{total}}] = \mathbb{E}[\xi] \mathbb{E}[N_j]$, is

$$\mathbb{E}[\xi_{j,\text{total}}] = \mathbb{E}[\xi] \mathbb{E}_S[\mathbb{E}[N_j | S]] = \mathbb{E}[\xi] \frac{\lambda_u}{\lambda_b}. \quad (8)$$

The variance of the total arrival rate in the area S_j is $\mathbb{D}[\xi_{j,\text{total}}] = \mathbb{E}[\xi_{j,\text{total}}^2] - (\mathbb{E}[\xi_{j,\text{total}}])^2$.

Let $D_{P,\xi_{j,\text{total}}}$ be the variance of total arrival rate in the uniformly distributed case, and $D_{C,\xi_{j,\text{total}}}$ be the variance of total arrival rate in the non-uniformly distributed case. With the above obtained mean total arrival rate, we obtain the following lemma.

Lemma 4. The variance in the uniformly distributed case is

$$D_{P,\xi_{j,\text{total}}} \approx (\mathbb{E}[\xi])^2 \left(0.2857 \frac{\lambda_u^2}{\lambda_b^2} + \frac{\lambda_u}{\lambda_b} \right). \quad (9)$$

The variance in the non-uniformly distributed case is

$$D_{C,\xi_{j,\text{total}}} \approx (\mathbb{E}[\xi])^2 \left(0.2857 \frac{\lambda_u^2}{\lambda_b^2} + \frac{\lambda_u}{\lambda_b} (\pi r_c^2 \lambda_c + 1) \right). \quad (10)$$

Proof: When the users are distributed as a PPP, the variance of the total arrival rate is

$$\begin{aligned} D_{P,\xi_{j,\text{total}}} &= \mathbb{E}[\xi_{j,\text{total}}^2] - (\mathbb{E}[\xi_{j,\text{total}}])^2 \\ &= \mathbb{E}_{S_j}[\mathbb{E}_{P,\xi_{j,\text{total}}}^2] - \left(\mathbb{E}[\xi] \frac{\lambda_u}{\lambda_b} \right)^2. \end{aligned} \quad (11)$$

In (11), the mean $\mathbb{E}_{P,\xi_{j,\text{total}}}$ is

$$\begin{aligned} \mathbb{E}_{P,\xi_{j,\text{total}}} &= \mathbb{E}[(\mathbb{E}[\xi])^2 N_j^2] \\ &= (\mathbb{E}[\xi])^2 \sum_{k=0}^{\infty} k^2 \mathbb{P}(N_j = k) \\ &\stackrel{(a)}{=} (\mathbb{E}[\xi])^2 (\lambda_u^2 S^2 + \lambda_u S), \end{aligned} \quad (12)$$

where (a) follows from the result

$$\begin{aligned} \sum_{k=0}^{\infty} k^2 \mathbb{P}(N_j = k) &= \sum_{k=0}^{\infty} k^2 \frac{e^{-\lambda_u S}}{k!} (\lambda_u S)^k \\ &= e^{-\lambda_u S} \lambda_u S \sum_{k=0}^{\infty} k \frac{(\lambda_u S)^{k-1}}{(k-1)!} \\ &= \lambda_u^2 S^2 + \lambda_u S. \end{aligned} \quad (13)$$

Plugging (12) into the equation (11), we get the variance of the total arrival rate as

$$\begin{aligned} D_{P,\xi_{j,\text{total}}} &\stackrel{(a)}{=} (\mathbb{E}[\xi])^2 \left(\int_0^{\infty} (\lambda_u^2 x^2 + \lambda_u x) f_{S_j}(x) dx - \frac{\lambda_u^2}{\lambda_b^2} \right) \\ &\stackrel{(b)}{\approx} (\mathbb{E}[\xi])^2 \left(0.2857 \frac{\lambda_u^2}{\lambda_b^2} + \frac{\lambda_u}{\lambda_b} \right), \end{aligned} \quad (14)$$

where (a) follows from the PDF of S_j , and (b) follows from the definition of $f_{S_j}(\cdot)$ given by (3) and the calculation of the integral as follows.

$$\begin{aligned}
& \int_0^\infty (\lambda_u^2 x^2 + \lambda_u x) f_{S_j}(x) dx \\
&= \int_0^\infty (\lambda_u^2 x^2 + \lambda_u x) \frac{343}{15} \sqrt{\frac{3.5}{\pi}} (x \lambda_b)^{2.5} e^{-3.5 \lambda_b x} \lambda_b dx \\
&\stackrel{(a)}{=} \frac{343}{15} \sqrt{\frac{3.5}{\pi}} \lambda_b^{3.5} \left(\lambda_u^2 \frac{\Gamma(5.5)}{(3.5 \lambda_b)^{5.5}} + \lambda_u \frac{\Gamma(4.5)}{(3.5 \lambda_b)^{4.5}} \right) \\
&\approx 1.2857 \frac{\lambda_u^2}{\lambda_b^2} + \frac{\lambda_u}{\lambda_b}, \tag{15}
\end{aligned}$$

where (a) follows from the integral $\int_0^\infty x^m e^{-\beta x^n} dx = \frac{\Gamma(r)}{n \beta^r}$, $r = \frac{m+1}{n}$. $\Gamma(x) = \int_0^\infty t^{x-1} e^{-t} dt$ denotes the standard gamma function.

When the users are distributed as a PCP, the variance of the total arrival rate is

$$D_{C, \xi_j, \text{total}} = \mathbb{E}_{S_j} [\mathbb{E}_{C, \xi_j, \text{total}}] - \left(\mathbb{E}[\xi] \frac{\lambda_u}{\lambda_b} \right)^2. \tag{16}$$

In the above equation (16), the mean $\mathbb{E}_{C, \xi_j, \text{total}}$ is

$$\mathbb{E}_{C, \xi_j, \text{total}} = (\mathbb{E}[\xi])^2 \mathbb{E}[N_j^2] = (\mathbb{E}[\xi])^2 \left(\mathbb{D}[N_j] + (\mathbb{E}[N_j])^2 \right), \tag{17}$$

where $N_j = \sum_{i=1}^{N_p} N_{C_i}$ is a Compound Poisson random variable and $N_{C_i} = \tilde{N}_{d_i}$ is the number of users in the i th cluster. According to the properties of Compound Poisson random variable, we have $\mathbb{E}[N_j] = \mathbb{E}[N_p] \mathbb{E}[N_C]$ and $\mathbb{D}[N_j] = \mathbb{E}[N_p] \left(\mathbb{D}[N_C] + (\mathbb{E}[N_C])^2 \right)$. N_p and N_C are Poisson random variable with mean $S \lambda_p$ and $\pi r_c^2 \lambda_c$, respectively. Therefore, the mean and variance of N_C is $\mathbb{D}[N_C] = \mathbb{E}[N_C] = \pi r_c^2 \lambda_c$, and the mean of N_p is $\mathbb{E}[N_p] = S \lambda_p$.

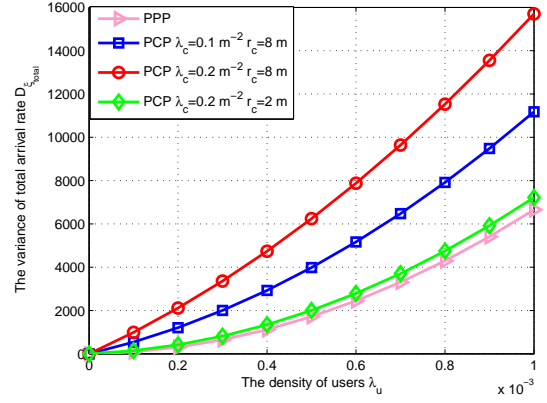
Then, the equation (17) can be derived as

$$\begin{aligned}
\mathbb{E}_{C, \xi_j, \text{total}} &= (\mathbb{E}[\xi])^2 \left(\mathbb{E}[N_p] \mathbb{D}[N_C] + \mathbb{E}[N_p] (\mathbb{E}[N_C])^2 \right. \\
&\quad \left. + (\mathbb{E}[N_p] \mathbb{E}[N_C])^2 \right). \tag{18}
\end{aligned}$$

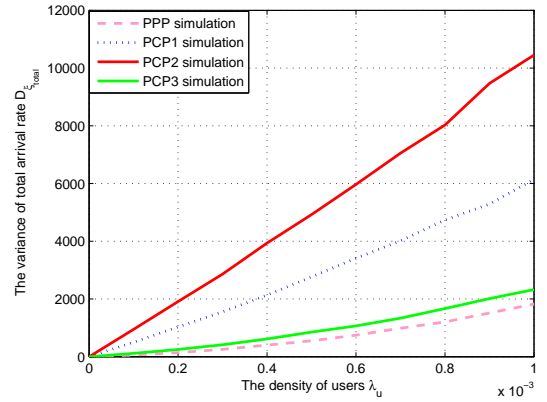
Similar to that in (14), we have

$$D_{C, \xi_j, \text{total}} \approx (\mathbb{E}[\xi])^2 \left(0.2857 \frac{\lambda_u^2}{\lambda_b^2} + \frac{\lambda_u}{\lambda_b} (\pi r_c^2 \lambda_c + 1) \right). \tag{19}$$

In Figure 7, we plot the variances of total arrival rate in a given area S for the uniformly and non-uniformly cases. We observe that the variance of total arrival rate increases when λ_u increases. This is because when the number of users increases, the difference of the arrival rate among the users will be greater. In particular, we observe that the variance of total arrival rate is larger in the non-uniformly distributed case than that in the uniformly distributed case. We also compare the variance in the non-uniformly distributed case for different r_c and λ_c . When fixing the radius of cluster r_c , the variance of the total arrival rate increases with the increase of the density of the clusters λ_c . When fixing the density of the clusters λ_c ,



(a) Numerical results



(b) Simulation results

Fig. 7. The variances of the total arrival rate in a given area S for the uniformly and non-uniformly distributed cases ($\lambda_b = 0.00001 m^{-2}$, $\mathbb{E}[\xi] = 1.5$).

the variance of the total arrival rate increases with the increase of the radius of cluster r_c . The reason is that when increasing the number of users in a cluster, the difference of the arrival rates also increases.

IV. SUCCESS PROBABILITY, ACHIEVABLE RATE AND DELAY

In this section, we analyze the effect of traffic on the success probability, achievable rate and delay. Since the network is static, i.e., the deployment of BSs is generated first and keeps unchanged hereafter, the success probabilities of various links are different, which results in different achievable rates and delays for different users.

We consider a typical user at the origin and the typical BS located at y_0 associated with the typical user. Let l be the distance between the typical user at the origin and the nearest BS y_0 . The PDF of l can be derived according to a simple fact that the null probability of a 2-D Poisson process in an area A is $e^{-\lambda_b A}$. Thus, the PDF of l is [19]

$$f_l(l) = 2\pi \lambda_b l e^{-\lambda_b \pi l^2}. \tag{20}$$

Here, the distance l is assumed to be a random variable and the result will be used in the following. A similar model is described by a meta distribution in [15].

The status of BSs in the network can be either busy or idle. We assume that the probability of each interfering BS being busy is q in each time slot t and the SIR at the typical user in the time slot t is denoted by SIR_t . Then, the SIR_t can be described as

$$\text{SIR}_t = \frac{P_b h_0 l_0^{-\alpha}}{\sum_{y_i \in \Phi_b \setminus y_0} \mathbb{I}_{y_i} P_b g_i L_i^{-\alpha}}, \quad (21)$$

where \mathbb{I}_{y_i} is the indicator function defined such that $\mathbb{I}_{y_i} = 1$, if the interfering BS y_i is active, and $\mathbb{I}_{y_i} = 0$, otherwise. Then, the probability of $\mathbb{I}_{y_i} = 1$ is q and the probability of $\mathbb{I}_{y_i} = 0$ is $1 - q$. The above result (21) can be obtained by (2). Here, the equation (21) presents the relationships between SIR_t and the typical link distance l_0 . When we calculate the expectation of BS deployment Φ_b , the distance l_0 should be regarded as a random variable.

A. Success Probability

In order to distinguish the SIRs in different time slots from (2), we keep the subscribe t in the following discussions. Then, the success probability conditioned on Φ_b is

$$\mathbf{P}_{s|\Phi_b} \triangleq \mathbf{P}(\text{SIR}_t > \theta | \Phi_b). \quad (22)$$

Since the interference depends on the path loss, the fading and the active probability, we have

$$I = \sum_{y_i \in \Phi_b \setminus y_0} \mathbb{I}_{y_i} P_b g_i L_i^{-\alpha}. \quad (23)$$

The active probability can be assumed to be the busy probability q , which is associated with the status of BS and if there are request packets arriving at the BS, the BS will be busy and the busy BS will result in the interference to other serving BS. The interference turns back to affect the arrival of packets and when the queue in the BS is empty, the BS will be idle and stop the interference to other BSs. Thus, the interference and the active probability are coupled.

In the random scheduling strategy, if there are N users within the considered cell, the typical BS will randomly choose one from the N users with probability $1/N$ in each time slot. For the typical user x_0 , the arrival rate of packets is ξ_0 , and the service rate (number of packets transmitted successfully per time slot) is $\mathbf{P}_{s|\Phi_b}/N$. According to the property of G/G/1 queue, conditioned on Φ_b , the probability that the queue at the user x_0 is not empty is

$$\mathbb{P}[\text{Queue is not empty} | \Phi_b] = \min \left\{ \frac{N\xi_0}{\mathbf{P}_{s|\Phi_b}}, 1 \right\}. \quad (24)$$

Since the probability of the typical BS being active equals the probability $\mathbb{P}[\text{Queue is not empty}]$. Thus, we get the active probability conditioned on Φ_b as

$$\mathbf{P}_{a|\Phi_b} = \min \left\{ \frac{N\xi_0}{\mathbf{P}_{s|\Phi_b}}, 1 \right\}. \quad (25)$$

The mean active probability is

$$\mathbf{P}_a = \mathbb{E}_{\Phi_b} \left[\min \left\{ \frac{N\xi_0}{\mathbf{P}_{s|\Phi_b}}, 1 \right\} \right] \stackrel{(a)}{\approx} \min \left\{ \frac{N\xi_0}{\mathbf{P}_s}, 1 \right\}, \quad (26)$$

where (a) is from the following approximation. $\frac{N\xi_0}{\mathbf{P}_{s|\Phi_b}}$ is a random variable, for simplify, denoted as X in the following. The expectation of X can be calculated as $\mathbb{E}(X)$. The expectation of $\min(X, 1)$ is $\min(\mathbb{E}(X), 1)$ in the approximation. When the traffic in the network is heavy, the active probability of the typical BS will approach to 1 at most time slots. In this case, the mean active probability is assumed to be 1. When the traffic is not heavy, the active probability of the typical BS can be regard as the set X where $X \leq 1$. In this case, the mean active probability is assumed to be $\mathbb{E}(X)$. Therefore, we made the approximation that the expectation of $\min(X, 1)$ is $\min(\mathbb{E}(X), 1)$. Since the busy probability of the typical BS q equals the mean active probability, we get a fixed-point equation as

$$\min \left\{ \frac{N\xi_0}{\mathbf{P}_s}, 1 \right\} = q, \quad (27)$$

where \mathbf{P}_s is given in Lemma 5.

Lemma 5. The solution of equation (27) can be expressed as

$$q^* = \begin{cases} \frac{N\xi_0 \text{sinc}(\delta)}{\text{sinc}(\delta) - N\xi_0 \theta^\delta}, & \text{if } 0 < \xi_0 < \frac{\text{sinc}(\delta)}{N(\text{sinc}(\delta) + \theta^\delta)} \\ 1, & \text{if } \xi_0 \geq \frac{\text{sinc}(\delta)}{N(\text{sinc}(\delta) + \theta^\delta)} \end{cases}. \quad (28)$$

where $\delta = 2/\alpha$ and $\text{sinc}(\cdot)$ is the sinc function.

Proof: Combined [17, eq.5.14] and [19], the conditional success probability is expressed as

$$\mathbf{P}_{s|l_0} = \exp \left(-\frac{\pi \lambda_b q \theta^\delta l_0^2}{\text{sinc}(\delta)} \right), \quad (29)$$

where the interference field is obtained by independent thinning of point process. Thus, the success probability can be evaluated as

$$\begin{aligned} \mathbf{P}_s &= \mathbb{E}_{l_0} [\mathbf{P}_{s|l_0}] = \int_0^\infty \exp \left(-\frac{\pi \lambda_b q \theta^\delta x^2}{\text{sinc}(\delta)} \right) f_{l_0}(x) dx \\ &= \frac{\text{sinc}(\delta)}{\text{sinc}(\delta) + q \theta^\delta}. \end{aligned} \quad (30)$$

Plugging \mathbf{P}_s into (27), the fixed-point equation (27) can be written as

$$\min \left\{ \frac{N\xi_0 (\text{sinc}(\delta) + q \theta^\delta)}{\text{sinc}(\delta)}, 1 \right\} = q. \quad (31)$$

In order to solve the above equation (31), we consider two cases, $0 < \frac{N\xi_0 (\text{sinc}(\delta) + q \theta^\delta)}{\text{sinc}(\delta)} < 1$ and $\frac{N\xi_0 (\text{sinc}(\delta) + q \theta^\delta)}{\text{sinc}(\delta)} \geq 1$. In order to facilitate the understanding of the equation solving process, we give the geometric solution of the equation. In Figure 8, the red lines show the range of solution for equation (31) and the red dot indicates the intersection of the curve $q = \frac{N\xi_0 \text{sinc}(\delta)}{\text{sinc}(\delta) - N\xi_0 \theta^\delta}$ and straight line $q = 1$. The abscissa of the red dot is indicated by B_0 .

- Case 1: $0 < \frac{N\xi_0 (\text{sinc}(\delta) + q \theta^\delta)}{\text{sinc}(\delta)} < 1$. In this case, we have $0 < q < 1$ and $\frac{N\xi_0 (\text{sinc}(\delta) + q \theta^\delta)}{\text{sinc}(\delta)} = q$. The solution of (31) depends on the intersection of the curve y_1 and the

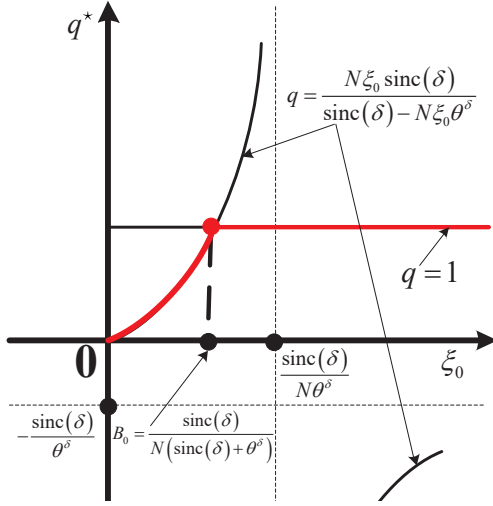


Fig. 8. Effect of the arrival rate of packets ξ_0 for the typical user on the active probability of the typical BS and the red lines show the range of solution for equation (31).

curve y_2 as shown in Figure 9. We get a conclusion, if $0 < \xi_0 < \frac{\text{sinc}(\delta)}{N(\text{sinc}(\delta) + \theta^\delta)}$, the solution of the equation is $q^* = \frac{N\xi_0 \text{sinc}(\delta)}{\text{sinc}(\delta) - N\xi_0 \theta^\delta}$; otherwise, the solution becomes $q^* = 1$ if $\xi_0 \geq \frac{\text{sinc}(\delta)}{N(\text{sinc}(\delta) + \theta^\delta)}$.

- Case 2: $\frac{N\xi_0(\text{sinc}(\delta) + q\theta^\delta)}{\text{sinc}(\delta)} \geq 1$. In this case, the solution is $q^* = 1$, and we get the other conclusion, if $\xi_0 \geq \frac{\text{sinc}(\delta)}{N(\text{sinc}(\delta) + \theta^\delta)}$, $q^* = 1$.

Thus, we obtain the solution of the fix-point equation (27) as shown in (28). ■

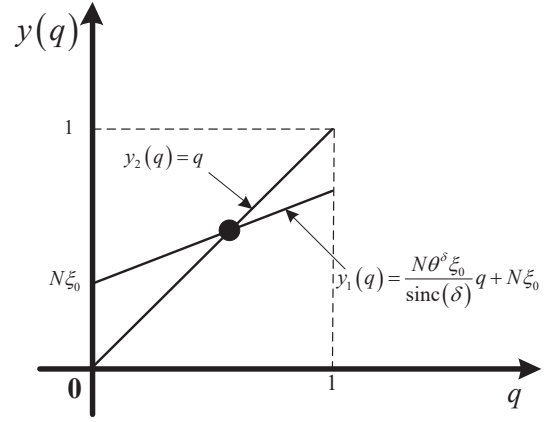
According to (28) and (30), the approximated success probability of the typical user is

$$\tilde{P}_s = \begin{cases} 1 - \frac{N\xi_0\theta^\delta}{\text{sinc}(\delta)}, & \text{if } 0 < \xi_0 < \frac{\text{sinc}(\delta)}{N(\text{sinc}(\delta) + \theta^\delta)} \\ \frac{\text{sinc}(\delta)}{\text{sinc}(\delta) + \theta^\delta}, & \text{if } \xi_0 \geq \frac{\text{sinc}(\delta)}{N(\text{sinc}(\delta) + \theta^\delta)} \end{cases}. \quad (32)$$

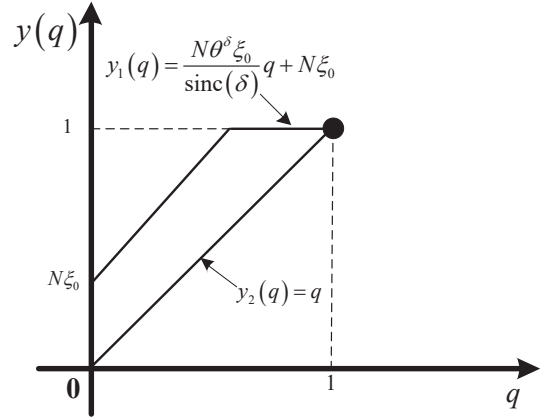
From the above expression, we observe that the approximated success probability is not only related to the path loss exponent but also related to the distribution of users and the threshold of SIR. By analyzing the expression (32), several observations can be obtained as follows.

1) When the arrival rate of the packets satisfies the condition $0 < \xi_0 < B_0$, the success probability is related to the path loss exponent, the distribution of users and the threshold of SIR. When ξ_0 or N increases, the success probability will decrease. This is because the success probability will decrease due to the competition increase of the users requesting service. When the path loss exponent increases, the success probability will increase, which is attributed to the less competition due to the decrease of the messages of service requests. As the threshold increases, the success probability decreases gradually. This is because the communication requirements are higher but the communication conditions are unchanged.

2) When the arrival rate of the packets satisfies the condition $\xi_0 \geq B_0$, the success probability is only related to the path loss



(a) When $0 < \xi_0 < \frac{\text{sinc}(\delta)}{N(\text{sinc}(\delta) + \theta^\delta)}$.



(b) When $\xi_0 \geq \frac{\text{sinc}(\delta)}{N(\text{sinc}(\delta) + \theta^\delta)}$.

Fig. 9. Curves of y_1 and y_2 in two cases for the equation (31).

exponent and the threshold of SIR. As the path loss exponent increases, the success probability will increase gradually and reach a maximum value. It implies that the interferences from other BSs are dominant when the arrival rate is large enough, and the effects of path loss on the interferences are larger than those on the signal.

B. Achievable Rate

In the following, we derive the achievable rate (bps/Hz) for the typical user x_0 . Since the packet size is fixed and a BS requires one time slot to deliver one packet, the achievable rate is

$$\tau = P_s \frac{L_p}{B \cdot \Delta t}, \quad (33)$$

where L_p is the length of one packet, B is the bandwidth and Δt is the length of one time slot.

In order to derive a closed-form expression of the mean rate, we normalize the bandwidth and the number of packets transmitted in the communication links is assumed to equal $\log_2(1 + \theta)$ in each second, i.e., $\frac{L_p}{B \cdot \Delta t} = \log_2(1 + \theta)$. There-

fore, by utilizing (32), we get the achievable rate for the typical user x_0 which is

$$\tau = \begin{cases} \frac{(\text{sinc}(\delta) - N\xi_0\theta^\delta)\log_2(1+\theta)}{\text{sinc}(\delta)}, & \text{if } 0 < \xi_0 < \frac{\text{sinc}(\delta)}{N(\text{sinc}(\delta) + \theta^\delta)} \\ \frac{\text{sinc}(\delta)\log_2(1+\theta)}{\text{sinc}(\delta) + \theta^\delta}, & \text{if } \xi_0 \geq \frac{\text{sinc}(\delta)}{N(\text{sinc}(\delta) + \theta^\delta)} \end{cases} \quad (34)$$

Observing the equation (34), we can find that the achievable rate is related to the path loss exponent, the distribution of users and the threshold of SIR. The achievable rate decreases linearly with N or ξ_0 , for $0 < \xi_0 < B_0$. The linear decrease comes from the increase of users service requests. When the arrival rate of the packets satisfies the condition $\xi_0 \geq B_0$, the achievable rate will only related to the path loss exponent and the threshold of SIR, which means the BS reaches its maximum capacity and the BS will be active all the time.

In Figure 10, we plot the achievable rate τ with respect to the SIR threshold θ (dB) for different path loss exponents and arrival rates of packets. As it can be observed from the curves, it seems counterintuitive that the achievable rate increases when the path loss exponent increases. The increase comes from the increase of success probability, and it means that the large path loss exponent is not always bad for the achievable rate. When the threshold of SIR $\theta < 0$, the achievable rate is very small and has similar trends in all curves. This is because the low threshold results in the huge competition due to almost all users in coverage area request service at the same time slot. The achievable rate initially increases along with the increase of threshold and reaches a peak value, but it starts to decrease as the threshold continue to increase and will tend to 0 as $\theta \rightarrow \infty$. In this case, the achievable rate is decided by both the first and last half of (34). The trend means that the threshold of SIR is not always opposite with the achievable rate and the appropriate increase of the threshold of SIR can help improve the achievable rate.

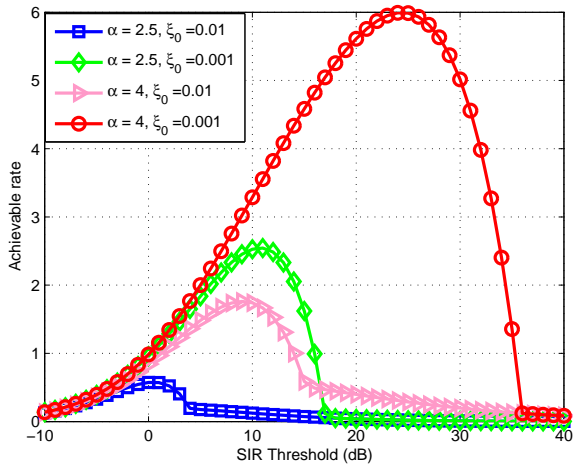


Fig. 10. Achievable rates for different path loss exponents and arrival rates of packets. The number of users is 10.

C. Statistic of Delay

In the following, we discuss the mean delay for random scheduling policy and analyze the relationship between the delay performance and the traffic.

In the random scheduling, the average rate of the typical user, denoted by $\mu = \bar{\mathbf{P}}_s/N$, is

$$\mu = \begin{cases} \frac{\text{sinc}(\delta) - N\xi_0\theta^\delta}{N\text{sinc}(\delta)}, & \text{if } 0 < \xi_0 < \frac{\text{sinc}(\delta)}{N(\text{sinc}(\delta) + \theta^\delta)} \\ \frac{\text{sinc}(\delta)}{N(\text{sinc}(\delta) + \theta^\delta)}, & \text{if } \xi_0 \geq \frac{\text{sinc}(\delta)}{N(\text{sinc}(\delta) + \theta^\delta)} \end{cases} \quad (35)$$

Attentively, we use the number of all users in the cell instead of the number of active users when calculating the service rate μ because it will alleviate the mathematical derivation and the delay is obtained in the rigorous circumstance. Therefore, the delay is the upper bound of the delay in the random scheduling. Due to the independence of the transmissions in different time slots, the probability for successfully transmitting a packet in any time slot can be considered as μ . Thus, the queueing system at the typical transmitter is a discrete-time Geo/G/1 queue in which the retrial time has a general distribution, and the server begins to search the next customer to serve [41] after each service completion.

In the equivalent Geo/G/1 queue, the arrival process of packets is a geometric arrival process since it is a Bernoulli process. The service rate is μ and the service times of the packets are i.i.d. with geometric distribution.

Theorem 1. In random scheduling, the mean delay \mathbf{D}_{ξ_0} can be expressed as

$$\mathbf{D}_{\xi_0} = \begin{cases} \frac{(1-\xi_0)N\text{sinc}(\delta)}{\text{sinc}(\delta) - N\xi_0\theta^\delta - N\xi_0\text{sinc}(\delta)}, & \text{if } N < \frac{\text{sinc}(\delta)}{\xi_0\text{sinc}(\delta) + \xi_0\theta^\delta} \\ \infty, & \text{if } N \geq \frac{\text{sinc}(\delta)}{\xi_0\text{sinc}(\delta) + \xi_0\theta^\delta} \end{cases} \quad (36)$$

Proof: From [41, Corollary 2 eq.7], the mean time that a customer spends in the system is

$$W = \beta_1 + \frac{2\bar{p}(\beta_1 - 1)[1 - A(\bar{p})] + p\beta_2}{2[p + \bar{p}A(\bar{p}) - \rho]}, \quad (37)$$

where β_n is the n th factorial moment of service rate, p is the arrival rate ($\bar{p} = 1 - p$), $\rho = p\beta_1$ is the traffic intensity, $A(x) = \sum_{i=0}^{\infty} a_i x^i$ is the Ordinary generating function of successive interretrial times of any user with an arbitrary distribution $\{a_i\}_{i=0}^{\infty}$. The retrial time is 0 in our queue system, so we have $a_0 = 1, a_{i \geq 1} = 0$ and $A(\bar{p}) = 1$. The service rate follows from geometric distribution. Combined with our own queue system, we get $\beta_1 = 1/\mu$, $\beta_2 = 2/\mu^2 - 2/\mu$, $p = \xi_0$, $A(\bar{p}) = 1$ and $\rho = p\beta_1$. By utilizing the above formulas, we get the mean delay as

$$\mathbf{D}_{\xi_0} = \begin{cases} \frac{1 - \xi_0}{\mu - \xi_0}, & \text{if } \mu > \xi_0 \\ \infty, & \text{if } \mu \leq \xi_0 \end{cases} \quad (38)$$

Plugging (35) into (38), we get the result in (36). ■

When the mean delay is finite and $\mathbf{D}_{\xi_0} < \beta$, we get the following inequality

$$\frac{(1 - \xi_0) N \text{sinc}(\delta)}{\text{sinc}(\delta) - N \xi_0 \theta^\delta - N \xi_0 \text{sinc}(\delta)} < \beta. \quad (39)$$

After simplifying the above inequality, we obtain

$$N < \frac{\text{sinc}(\delta)}{\frac{1}{\beta}(1 - \xi_0) \text{sinc}(\delta) + (\xi_0 \theta^\delta + \xi_0 \text{sinc}(\delta))}. \quad (40)$$

In order to facilitate the above expression, we define

$$A_1 = \frac{\text{sinc}(\delta)}{\xi_0 \theta^\delta + \xi_0 \text{sinc}(\delta)}, \quad (41)$$

$$A_2 = \frac{\text{sinc}(\delta)}{\frac{1}{\beta}(1 - \xi_0) \text{sinc}(\delta) + (\xi_0 \theta^\delta + \xi_0 \text{sinc}(\delta))}, \quad (42)$$

where $A_1 > A_2$ and β is the delay requirement of the typical user.

By analyzing the above inequalities, we obtain several conclusions as follows.

1) When the number of users N satisfies $N < A_2$, the queue is stable, and the delay requirement can be satisfied. By observing the expression of A_2 , we obtain that the larger the value of β is, the greater the value that N will be. In other words, when the delay requirements are low, the typical cell can accommodate more users and satisfies their delay requirements.

2) When N satisfies the condition $A_2 < N < A_1$, the queue is stable but the delay requirements of users can not be satisfied, i.e., the arriving users can be successfully served by the associated BS, but the delay requirements of users can not be met.

3) When N satisfies the condition $N > A_1$, the queue is not stable, i.e., the users will be blocked in the system and can not be successfully served by the associated BS.

V. UNSTABLE PROBABILITY

In this section, we analyze the unstable probability of the queue at the typical user, which reveals the stability performance of all queues in the wireless network.

Definition 1. In the Geo/G/1 queue, when the arrival rate of packets ξ_0 is less than the service rate of the system μ , the queue will be stable. The probability of the typical queue being stable can be regarded as the stability of the queues. The stable probability is defined as

$$\mathbf{P}_{\text{stable}} = \mathbb{P}(\xi_0 < \mu). \quad (43)$$

Therefore, the unstable probability, expressed as $\mathbf{P}_{\text{us}} = \mathbb{P}(\xi_0 \geq \mu)$, can be evaluated as follows.

Theorem 2. The unstable probability of the typical queue in the network is

$$\mathbf{P}_{\text{us}} = 1 - \sum_{k=1}^{\infty} \mathbb{P}(\xi_0 \leq f(k)) \mathbb{P}(N = k) - \mathbb{P}(N = 0), \quad (44)$$

where $f(k) = \frac{\text{sinc}(\delta)}{k(\text{sinc}(\delta) + \theta^\delta)}$ and $\mathbb{P}(N = k)$ is the PMF of N given by (4) and (5).

Proof: According to (36), the unstable probability can be derived explicitly as

$$\begin{aligned} \mathbf{P}_{\text{us}} &= \mathbb{P}\left(N \geq \frac{\text{sinc}(\delta)}{\xi_0(\text{sinc}(\delta) + \theta^\delta)}\right) \\ &= 1 - \sum_{k=1}^{\infty} \mathbb{P}(\xi_0 \leq f(k)) \mathbb{P}(N = k) - \mathbb{P}(N = 0), \end{aligned} \quad (45)$$

where $\mathbb{P}(\xi_0 \leq f(k))$ can be evaluated by the cumulative distribution function of ξ_0 and $\mathbb{P}(N = k)$ can be obtained by (4) or (5). ■

Since the arrival rate of the packets ξ_0 may obey different distribution, we consider the unstable probability under exponential distribution and uniform distribution, respectively.

First, we consider the arrival rate $\xi_0 \sim E(\lambda)$, the unstable probability can be derived as

$$\begin{aligned} \mathbf{P}_{\text{us}} &= 1 - \sum_{k=1}^{\infty} \left(1 - \exp\left(-\frac{\lambda \text{sinc}(\delta)}{k(\text{sinc}(\delta) + \theta^\delta)}\right)\right) \mathbb{P}(N = k) \\ &\quad - \mathbb{P}(N = 0). \end{aligned} \quad (46)$$

When the arrival rate satisfies $\xi_0 \sim U(0, b)$, the unstable probability can be written as

$$\begin{aligned} \mathbf{P}_{\text{us}} &= 1 - \sum_{k=a}^{\infty} \left(\frac{\text{sinc}(\delta)}{kb(\text{sinc}(\delta) + \theta^\delta)}\right) \mathbb{P}(N = k) \\ &\quad - \sum_{k=0}^{a-1} \mathbb{P}(N = k), \end{aligned} \quad (47)$$

where the condition is $\frac{\text{sinc}(\delta)}{a(\text{sinc}(\delta) + \theta^\delta)} \leq b < \frac{\text{sinc}(\delta)}{(a-1)(\text{sinc}(\delta) + \theta^\delta)}$.

When $\xi_0 \sim E(\lambda)$ and the users form a PPP, combined (4) with (46), we get

$$\mathbf{P}_{\text{us}} = 1 - \sum_{k=1}^{\infty} \left(1 - e^{-\frac{\lambda \text{sinc}(\delta)}{k(\text{sinc}(\delta) + \theta^\delta)}}\right) \frac{e^{-\lambda_u S}}{k!} (\lambda_u S)^k - e^{-\lambda_u S}. \quad (48)$$

When the users are distributed as a PCP, combined (5) with (46), the unstable probability is

$$\begin{aligned} \mathbf{P}_{\text{us}} &= 1 - \sum_{k=1}^{\infty} \left(\left(1 - e^{-\frac{\lambda \text{sinc}(\delta)}{k(\text{sinc}(\delta) + \theta^\delta)}}\right) \right. \\ &\quad \times \left. \left(\sum_{a=0}^{\infty} \frac{e^{-\lambda_p S}}{a!} (\lambda_p S e^{-\lambda_c \pi r_c^2})^a \frac{(\lambda_c a \pi r_c^2)^k}{k!} \right) \right) \\ &\quad - \exp\left((e^{-\lambda_c \pi r_c^2} - 1) \lambda_p S\right). \end{aligned} \quad (49)$$

When $\xi_0 \sim U(0, b)$ and the users form a PPP, combined (4) with (47), we get

$$\begin{aligned} \mathbf{P}_{\text{us}} &= 1 - \sum_{k=m}^{\infty} \left(\frac{\text{sinc}(\delta)}{kb(\text{sinc}(\delta) + \theta^\delta)}\right) \frac{e^{-\lambda_u S}}{k!} (\lambda_u S)^k \\ &\quad - \sum_{k=0}^{m-1} \frac{e^{-\lambda_u S}}{k!} (\lambda_u S)^k. \end{aligned} \quad (50)$$

Similarly, when the users are distributed as a PCP, combined (5) with (47), we get

$$\begin{aligned} P_{us} = 1 - \sum_{k=m}^{\infty} \left(\left(\frac{\text{sinc}(\delta)}{kb(\text{sinc}(\delta) + \theta^\delta)} \right) \right. \\ \times \left(\sum_{a=0}^{\infty} \frac{e^{-\lambda_p S}}{a!} \left(\lambda_p S e^{-\lambda_c \pi r_c^2} \right)^a \frac{(\lambda_c a \pi r_c^2)^k}{k!} \right) \\ \left. - \sum_{k=0}^{m-1} \left(\sum_{a=0}^{\infty} \frac{e^{-\lambda_p S}}{a!} \left(\lambda_p S e^{-\lambda_c \pi r_c^2} \right)^a \frac{(\lambda_c a \pi r_c^2)^k}{k!} \right) \right). \end{aligned} \quad (51)$$

The numerical results of unstable probability are shown in Figure 12, Figure 13 and Figure 14.

VI. NUMERICAL EVALUATION

In this section, we numerically evaluate the delay and the stability which validates the claims in the above discussions and help to gain insights.

A. Delay Performance

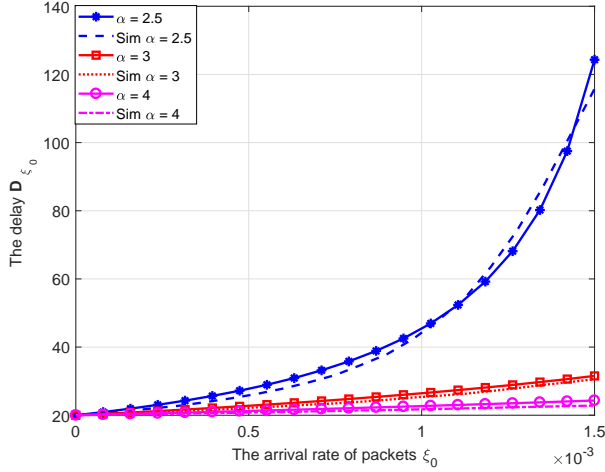


Fig. 11. Effect of the arrival rate ξ_0 on the conditional mean delay D_{ξ_0} for different α ($N = 20, \theta = 10$).

In Figure 11, we plot the conditional mean delay D_{ξ_0} given by (36) with respect to the arrival rate of packets ξ_0 for different path loss exponents. We observe that, when the value of ξ_0 is small, as ξ_0 increases, the conditional mean delay D_{ξ_0} increases gradually since the waiting time is longer due to the increase of the number of arrival packets in a slot time. When the value of ξ_0 is larger than a certain value, the conditional mean delay D_{ξ_0} will be infinite which means that the queue is unstable. This can be interpreted as that the service ability of BSs are limited and the system will be blocked when the traffic is overloaded in each time slot. As the path loss exponent α increases, the conditional mean delay D_{ξ_0} decreases since the waiting time is shorter due to the decrease of the number of arrival packets.

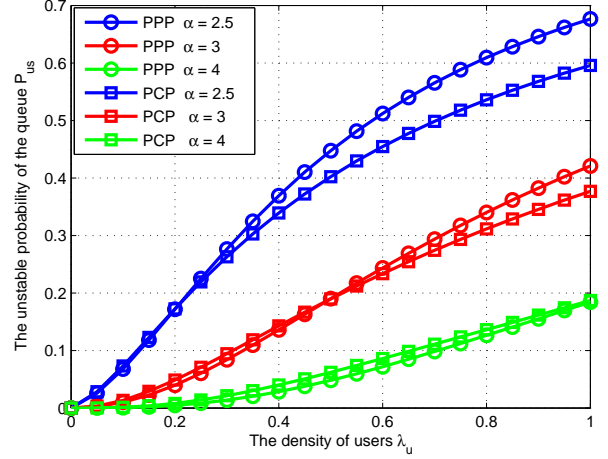


Fig. 12. Effect of the density of users λ_u on the unstable probability P_{us} for different path loss exponents α and various distributions of users when the arrival rate follows an exponential distribution with mean 0.01. The parameters are set as $\theta = 10, S = 10, r_c = 1, \lambda_p = \frac{1}{1.1\pi}$ and $\lambda_c = 1.1\lambda_u$.

B. Unstable Probability

In Figure 12, we plot the unstable probability P_{us} given by (46) as functions of the density of users λ_u for different path loss exponents α . The arrival rate of packets ξ_0 follows an exponential distribution with mean 0.01. As the density of users λ_u increases, the unstable probability P_{us} increases due to the increase of the number of users in a given area S . When the density of users λ_u increases to a large value, the unstable probability P_{us} will approach to 1. It means that the BS reaches its maximum accommodation capacity and the users cannot be served successfully by the BS in this case. However, as the path loss exponent α increases, the unstable probability P_{us} decreases gradually since the loss of packets at the communication links will reduce the number of packets arriving the queue and further reduce the unstable probability of the queue. Noted that, when the density of users λ_u is very small, the unstable probability in the uniformly distributed case is less than that in the non-uniformly distributed case for the same λ_u . When the density of users continues to increase, the unstable probability in the uniformly distributed case will exceed that in the non-uniformly distributed case. Thus, when the arrival rate follows an exponential distribution, the stability of queue in the uniformly distributed case is better than that in the non-uniformly distributed case for small λ_u , and it is reversed for large λ_u .

In Figure 13, we plot the unstable probability P_{us} given by (47) as functions of the density of users λ_u for different path loss exponents α . The arrival rate of packets ξ_0 follows a continuous uniform distribution denoted by $U(0, 0.02)$. Similar to the results in Figure 12, as the density of users λ_u increases, the unstable probability P_{us} increases, and as the path loss exponent α increases, the unstable probability P_{us} decreases. We can observe a similar trend for the unstable probability as that in Figure 12. It further verifies the conclusion that the stability of queue in the uniformly distributed case is better than that in the non-uniformly distributed case for small λ_u ,

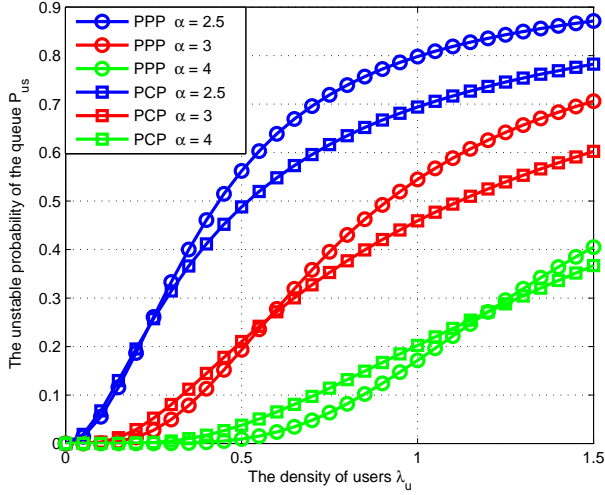


Fig. 13. Effect of the density of users λ_u on the unstable probability P_{us} for different path loss exponents α and various distributions of users when the arrival rate follows a continuous uniform distribution denoted by $U(0, 0.02)$. The parameters are set as $\theta = 10$, $S = 10$, $r_c = 1$, $\lambda_p = \frac{1}{1.1\pi}$ and $\lambda_c = 1.1\lambda_u$.

and it is reversed for large λ_u . When the density of users is small, the active BSs in PCP will be more than those in PPP because the users in PCP are more concentrated, and there will be more users in some cells and less users in other cells. The users in PPP are uniformly scattered. Since the active probability of the BSs with more users will be larger, the number of active BSs in PCP will be larger than that in PPP. The more BSs being active, the more interference will be generated in the network, which leads to the deterioration of the stability performance of queues. Contrast with Figure 12, we observe that the unstable probabilities in Figure 13 are larger than those in Figure 12 when changing the distribution of ξ_0 , indicating that the stability performance of queues is better when the arrival rate ξ_0 follows an exponential distribution.

In Figure 14, we plot the unstable probability P_{us} given by (46) and (47) as functions of the density of users λ_u for different PCP parameters and various distributions of arrival rate. The arrival rate of packets ξ_0 follows a continuous uniform distribution denoted by $U(0, 1)$ or an exponential distribution with mean 0.5. The unstable probability in PCP 1 is larger than that in PCP 2 when $\lambda_u < 1$, which means the users in PCP 2 are more likely to be served successfully than those in PCP 1. This is because when the distribution is PCP 1, the number of users experiencing strong interference will increase drastically which leads to the increase of the unstable probability. When the user distribution is PCP 2, the probability that the users experiencing strong interference is smaller and the unstable probability will also be smaller. The stability of queue is better when the ξ_0 follows an exponential distribution compared to it in $\xi_0 \sim U(0, 1)$. In particular, when the path loss exponent $\alpha = 2.5$, the interval shown in circle 1 is small, but when the path loss exponent is $\alpha = 4$, the interval shown in circle 2 is bigger. Therefore, when the density of users λ_u is medium, the stability of queue is not dominated by the distributions of ξ_0 but dominated by the path

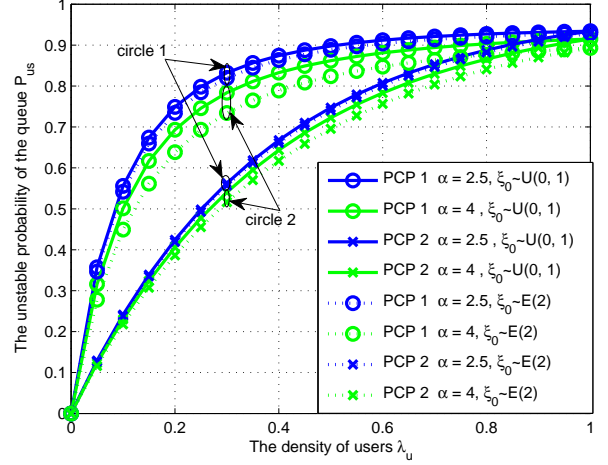


Fig. 14. Effect of the density of users λ_u on P_{us} for different path loss exponents α when the arrival rate follows either a continuous uniform distribution denoted by $U(0, 1)$ or an exponential distribution with mean 0.5. The parameters are set as $\theta = 10$, $S = 10$, $r_c = 1$, $\lambda_p = \frac{1}{1.1\pi}$, $\lambda_c = 1.1\lambda_u$ for PCP 1 and $\theta = 10$, $S = 10$, $r_c = 1$, $\lambda_p = \frac{\lambda_u}{1.1\pi}$, $\lambda_c = 1.1$ for PCP 2.

loss exponent.

VII. CONCLUSION

In this paper, we consider a tractable model to analyze the effect of spatio-temporal traffic on the wireless network. By considering a network consisting of one tier of BSs and one tier of users, we compared the distributions of users in the uniformly distributed case and the non-uniformly distributed case and derived the PMF of the number of users, the variance of total arrival rate, the success probability, the achievable rate, the conditional mean delay and the unstable probability of queue. Specific expressions were obtained for the proposed model. Based on the obtained expressions, we discussed the effect of spatio-temporal traffic on network delay and the stability performance of queues.

From the numerical evaluation, we observe that the fluctuations of total arrival rate are greater in the non-uniformly distributed case than that in the uniformly distributed case. The stability of queue in the non-uniformly distributed case is better than that in the uniformly distributed case when the density of users is large or when the arrival rate follows an exponential distribution. Our analyses reveal the differences between the uniformly and non-uniformly distributed traffic and provide insights on the design of wireless networks when various spatio-temporal properties of traffic is considered.

REFERENCES

- [1] G. Wang, Y. Zhong, T. Han, X. Ge, and T. Q. S. Quek, "On the Effect of Spatio-Temporal Fluctuation of Traffic in Wireless Networks," in *IEEE Global Communications Conference (GLOBECOM)*, Dec. 2018.
- [2] M. Simsek, A. Aijaz, M. Dohler, J. Sachs, and G. Fettweis, "5G-Enabled Tactile Internet," *IEEE J. on Sel. Areas in Commun.*, vol. 34, no. 3, pp. 460–473, Mar. 2016.
- [3] G. P. Fettweis, "The Tactile Internet: Applications and Challenges," *IEEE Vehicular Technology Magazine*, vol. 9, no. 1, pp. 64–70, Mar. 2014.

- [4] C. V. Mobile, "Global mobile data traffic forecast update 2010-2015," *Cisco White Paper*, 2011.
- [5] Y. Zhong, X. Ge, H. H. Yang, T. Han, and Q. Li, "Traffic Matching in 5G Ultra-Dense Networks," *IEEE Commun. Magazine*, vol. 56, no. 8, pp. 100–105, Aug. 2018.
- [6] D. Lee, S. Zhou, X. Zhong, Z. Niu, X. Zhou, and H. Zhang, "Spatial modeling of the traffic density in cellular networks," *IEEE Wireless Commun.*, vol. 21, no. 1, pp. 80–88, Feb. 2014.
- [7] H. Wang, J. Ding, Y. Li, P. Hui, J. Yuan, and D. Jin, "Characterizing the Spatio-Temporal Inhomogeneity of Mobile Traffic in Large-scale Cellular Data Networks," in *Proc. of the 7th International Workshop on Hot Topics in Planet-scale mObile Computing and Online Social neTworking*, ser. HOTPOST, 2015, pp. 19–24.
- [8] R. Li, Z. Zhao, J. Zheng, C. Mei, Y. Cai, and H. Zhang, "The Learning and Prediction of Application-Level Traffic Data in Cellular Networks," *IEEE Trans. on Wireless Commun.*, vol. 16, no. 6, pp. 3899–3912, June 2017.
- [9] Z. Niu, "TANGO: traffic-aware network planning and green operation," *IEEE Wireless Commun.*, vol. 18, no. 5, pp. 25–29, Oct. 2011.
- [10] F. Xu, Y. Li, H. Wang, P. Zhang, and D. Jin, "Understanding Mobile Traffic Patterns of Large Scale Cellular Towers in Urban Environment," *IEEE/ACM Trans. on Networking*, vol. 25, no. 2, pp. 1147–1161, Apr. 2017.
- [11] B. Cici, M. Gjoka, A. Markopoulou, and C. T. Butts, "On the Decomposition of Cell Phone Activity Patterns and Their Connection with Urban Ecology," in *Proceedings of the 16th ACM International Symposium on Mobile Ad Hoc Networking and Computing*, ser. MobiHoc. ACM, 2015, pp. 317–326.
- [12] Y. Zhong and W. Zhang, "Multi-Channel Hybrid Access Femtocells: A Stochastic Geometric Analysis," *IEEE Trans. on Commun.*, vol. 61, no. 7, pp. 3016–3026, July 2013.
- [13] S. Singh, H. S. Dhillon, and J. G. Andrews, "Offloading in Heterogeneous Networks: Modeling, Analysis, and Design Insights," *IEEE Trans. on Wireless Commun.*, vol. 12, no. 5, pp. 2484–2497, May 2013.
- [14] H. S. Jo, Y. J. Sang, P. Xia, and J. G. Andrews, "Heterogeneous Cellular Networks with Flexible Cell Association: A Comprehensive Downlink SINR Analysis," *IEEE Trans. on Wireless Commun.*, vol. 11, no. 10, pp. 3484–3495, Oct. 2012.
- [15] Y. Wang, M. Haenggi, and Z. Tan, "The Meta Distribution of the SIR for Cellular Networks With Power Control," *IEEE Trans. on Commun.*, vol. 66, no. 4, pp. 1745–1757, Apr. 2018.
- [16] M. Haenggi, J. G. Andrews, F. Baccelli, O. Dousse, and M. Franceschetti, "Stochastic geometry and random graphs for the analysis and design of wireless networks," *IEEE J. on Sel. Areas in Commun.*, vol. 27, no. 7, pp. 1029–1046, Sept. 2009.
- [17] M. Haenggi, *Stochastic geometry for wireless networks*. Cambridge University Press, 2012.
- [18] M. Afshang and H. S. Dhillon, "Poisson Cluster Process Based Analysis of HetNets With Correlated User and Base Station Locations," *IEEE Trans. on Wireless Commun.*, vol. 17, no. 4, pp. 2417–2431, Apr. 2018.
- [19] J. G. Andrews, F. Baccelli, and R. K. Ganti, "A Tractable Approach to Coverage and Rate in Cellular Networks," *IEEE Trans. on Commun.*, vol. 59, no. 11, pp. 3122–3134, Nov. 2011.
- [20] Z. Chen, N. Pappas, M. Kountouris, and V. Angelakis, "Throughput With Delay Constraints in a Shared Access Network With Priorities," *IEEE Trans. on Wireless Commun.*, vol. 17, no. 9, pp. 5885–5899, Sept. 2018.
- [21] N. Pappas, Z. Chen, and I. Dimitriou, "Throughput and Delay Analysis of Wireless Caching Helper Systems With Random Availability," *IEEE Access*, vol. 6, pp. 9667–9678, 2018.
- [22] I. Dimitriou and N. Pappas, "Stable Throughput and Delay Analysis of a Random Access Network With Queue-Aware Transmission," *IEEE Trans. on Wireless Commun.*, vol. 17, no. 5, pp. 3170–3184, May 2018.
- [23] R. R. Rao and A. Ephremides, "On the stability of interacting queues in a multiple-access system," *IEEE Trans. on Inform. Theory*, vol. 34, no. 5, pp. 918–930, Sept. 1988.
- [24] B. S. Tsybakov and V. A. Mikhailov, "Ergodicity of a slotted ALOHA system," *Problemy peredachi informatsii*, vol. 15, no. 4, pp. 73–87, 1979.
- [25] W. Szpankowski, "Stability conditions for some distributed systems: Buffered random access systems," *Advances in Applied Probability*, vol. 26, no. 02, pp. 498–515, 1994.
- [26] V. Anantharam, "The stability region of the finite-user slotted ALOHA protocol," *IEEE Trans. on Inform. Theory*, vol. 37, no. 3, pp. 535–540, May 1991.
- [27] W. Luo and A. Ephremides, "Stability of N interacting queues in random-access systems," *IEEE Trans. on Inform. Theory*, vol. 45, no. 5, pp. 1579–1587, 1999.
- [28] X. Ge, B. Yang, J. Ye, G. Mao, C.-X. Wang, and T. Han, "Spatial spectrum and energy efficiency of random cellular networks," *IEEE Trans. on Commun.*, vol. 63, no. 3, pp. 1019–1030, 2015.
- [29] L. Xiang, X. Ge, C.-X. Wang, F. Y. Li, and F. Reichert, "Energy efficiency evaluation of cellular networks based on spatial distributions of traffic load and power consumption," *IEEE Trans. on Wireless Commun.*, vol. 12, no. 3, pp. 961–973, 2013.
- [30] X. Ge, J. Ye, Y. Yang, and Q. Li, "User mobility evaluation for 5G small cell networks based on individual mobility model," *IEEE J. on Sel. Areas in Commun.*, vol. 34, no. 3, pp. 528–541, 2016.
- [31] N. Abbas, T. Bonald, and B. Sayrac, "How Mobility Impacts the Performance of Inter-Cell Coordination in Cellular Data Networks," in *IEEE Global Communications Conference (GLOBECOM)*, Dec. 2015.
- [32] N. Sapountzis, T. Spyropoulos, N. Nikaen, and U. Salim, "An Analytical Framework for Optimal Downlink-Uplink User Association in HetNets with Traffic Differentiation," in *IEEE Global Communications Conference (GLOBECOM)*, Dec. 2015.
- [33] Y. Zhong, T. Q. S. Quek, and X. Ge, "Heterogeneous Cellular Networks With Spatio-Temporal Traffic: Delay Analysis and Scheduling," *IEEE J. on Sel. Areas in Commun.*, vol. 35, no. 6, pp. 1373–1386, June 2017.
- [34] M. Gharbieh, H. ElSawy, A. Bader, and M. Alouini, "Spatiotemporal Stochastic Modeling of IoT Enabled Cellular Networks: Scalability and Stability Analysis," *IEEE Trans. on Commun.*, vol. 65, no. 8, pp. 3585–3600, Aug. 2017.
- [35] N. Jiang, Y. Deng, X. Kang, and A. Nallanathan, "Random Access Analysis for Massive IoT Networks Under a New Spatio-Temporal Model: A Stochastic Geometry Approach," *IEEE Trans. on Commun.*, vol. 66, no. 11, pp. 5788–5803, Nov. 2018.
- [36] J. Park, S. Y. Jung, S. Kim, M. Bennis, and M. Debbah, "User-Centric Mobility Management in Ultra-Dense Cellular Networks under Spatio-Temporal Dynamics," in *IEEE Global Communications Conference (GLOBECOM)*, Dec. 2016.
- [37] Y. Zhong, X. Ge, T. Han, Q. Li, and J. Zhang, "Tradeoff Between Delay and Physical Layer Security in Wireless Networks," *IEEE J. on Sel. Areas in Commun.*, vol. 36, no. 7, pp. 1635–1647, July 2018.
- [38] B. Błaszczyszyn, M. Jovanovic, and M. K. Karay, "Performance laws of large heterogeneous cellular networks," in *13th International Symposium on Modeling and Optimization in Mobile, Ad Hoc, and Wireless Networks (WiOpt)*, IEEE, 2015, pp. 597–604.
- [39] X. Zhou, Z. Zhao, R. Li, Y. Zhou, and H. Zhang, "The predictability of cellular networks traffic," in *International Symposium on Communications and Information Technologies (ISCIT)*, Oct. 2012, pp. 973–978.
- [40] J.-S. Ferenc and Z. Neda, "On the size distribution of Poisson Voronoi cells," *Physica A: Statistical Mechanics and its Applications*, vol. 385, no. 2, pp. 518–526, 2007.
- [41] I. Atencia and P. Moreno, "A Discrete-Time Geo/G/1 Retrial Queue with General Retrial Times," *Queueing Systems*, vol. 48, no. 1, pp. 5–21, Sept. 2004.